J|A|C|S COMMUNICATIONS

Published on Web 04/20/2009

Mössbauer, NMR, Geometric, and Electronic Properties in $S = {}^3/_2$ Iron Porphyrins

Yan Ling and Yong Zhang*

Departments of Chemistry and Biochemistry, University of Southern Mississippi, 118 College Drive #5043, Hattiesburg, Mississippi 39406

Received January 28, 2009; E-mail: yong.zhang@usm.edu

Iron porphyrins with the intermediate spin $S = {}^3/_2$ or admixed with $S = {}^5/_2$ or ${}^1/_2$ are models for a number of heme protein systems,[1,2] including cytochromes c′. They have been intensely investigated experimentally.[1−17] In particular, the ^{57}Fe Mössbauer quadrupole splittings and ^{1}H and ^{13}C NMR chemical shifts have been found to be useful probes of their electronic states. However, specific relationships between these spectroscopic properties and geometric parameters have not been reported. There are also no reports of quantum chemical calculations of these important spectroscopic probes in $S = {}^3/_2$ iron porphyrins, except for our recent work on the Mössbauer properties of one such complex.[18] In addition, their electronic states are under debate. While early work suggested an electronic configuration of $(d_{xy})^2(d_{xz}, d_{yz})^2(d_{z^2})^1(d_{x^2-y^2})^0$ for $S = {}^3/_2$ ferric porphyrins,[1] more recent experimental work[4] discovered two possibilities: the previously proposed electronic state for saddled iron porphyrins and a new electronic configuration of $(d_{xz}, d_{yz})^3(d_{xy})^1(d_{z^2})^1(d_{x^2-y^2})^0$ for ruffled ones. However, a recent theoretical study proposed an opposite assignment of these two electronic states.[19]

Here we present the results of the first quantum chemical calculations of the Mössbauer and NMR properties in various $S = {}^3/_2$ iron porphyrins and their interesting new correlations with geometric and electronic properties. As shown in Table 1, the $S = {}^3/_2$ complexes investigated here cover all of the possible coordination states of iron porphyrins (four-, five-, and six-coordinate) as well as the commonly seen porphyrin conformations (planar, ruffled, and saddled).[3−5,7,9−14,16,17] In addition to the almost pure $S = {}^3/_2$ complexes **1**, **3**, **4**, and **5**, one containing 20% $S = {}^5/_2$ (**2**) as well as one related to those having spin crossover with $S = {}^1/_2$ (**6**) were studied. A couple of spin-admixed complexes with mostly $S = {}^5/_2$ features (**7**, **8**) were also calculated for comparison. Experimental X-ray structures were used in all of the calculations, which used the density functional theory (DFT) method that previously gave accurate predictions of Mössbauer quadrupole splittings (ΔE_Q) and isomer shifts (δ_{Fe})[18,20] and NMR ^{1}H and ^{13}C hyperfine shifts[21] for metalloproteins and models.[22]

The data in Table 1 clearly show that the computational results support the experimental findings that the Mössbauer quadrupole splittings and ^{1}H and ^{13}C NMR hyperfine shifts are sensitive probes of the spin states ($S = {}^3/_2$ vs ${}^5/_2$ or ${}^1/_2$), since for each of these complexes, only the calculated results obtained using the correct spin state for the X-ray structure are in good agreement with the experimental spectroscopic data. As illustrated in Figure 1A, the calculated ΔE_Q results[3,10,12−14,17] have a theory-versus-experiment correlation coefficient of $R^2 = 0.99$ and a standard deviation of 0.12 mm/s or 2.9% of the whole experimental range from 0.95 to 5.16 mm/s. These results extend previous computational work on iron-containing proteins and models[18,20] to a total experimental range of 8.80 mm/s with $R^2 = 0.98$ (Figure S1 in the Supporting Information). The experimental Mössbauer isomer shifts were also well reproduced (Table 1). However, these data are insensitive to spin states and only display a small range (see Figure 1B), precluding the use of δ_{Fe} as a sensitive probe of these complexes. The ^{1}H NMR chemical shifts of pyrrole protons have long been recognized as good indicators of spin states in spin-admixed (${}^3/_2$, ${}^5/_2$) complexes[3,12,13,15] because of the different spin density distributions between the intermediate- and high-spin states, which affect the observed NMR hyperfine shifts ($\delta_{hf}^{H\beta}$), a major component of the NMR chemical shift that is proportional to the spin densities.[21,22] For porphyrins with substituents at the pyrrole proton positions, such as OEP and OETPP, the experimental NMR hyperfine shifts of the $-CH_2-$ group of the ethyl substituents[4,7,9,10] ($\delta_{hf}^{HC\alpha}$) were also investigated. As shown in Table 1 and Figure 1C, the experimental ^{1}H NMR hyperfine shifts, which cover a range of 122.7 ppm, were accurately predicted ($R^2 = 0.99$). The predicted ^{13}C NMR hyperfine shifts for the porphyrin α-, β-, and meso carbons ($\delta_{hf}^{C\alpha}$, $\delta_{hf}^{C\beta}$, and δ_{hf}^{Cm}, respectively) are also in good agreement with experiment. Overall, the NMR predictions for these $S = {}^3/_2$ systems fall on the same trend line as in previous calculations on proteins and models with other spin states[21] (Figure S2). These results provide a solid basis for the use of DFT calculations to investigate $S = {}^3/_2$ ferric porphyrin systems.

Since these results represent the first successful calculations of experimental Mössbauer and NMR properties for a good variety of $S = {}^3/_2$ iron porphyrins, we next investigated the relationships between these sensitive experimental probes and the structural features. Interestingly, the Mössbauer quadrupole splittings in these porphyrins (**1**−**8**) were found for the first time to have good correlations with the average length of the bonds between the iron and the pyrrole nitrogen (R_{FeN}). Although most of the complexes studied here have intermediate spin and only two have high spin, this correlation can also be extended to other high-spin iron porphyrins and heme protein[18] (**9**−**12**, Table S2). As depicted in Figure 1D, large quadrupole splittings are correlated with smaller Fe−N bond lengths ($R^2 = 0.93$), and this correlation is independent of coordination state and porphyrin conformation. It should be noted that the Mössbauer quadrupole splittings are also correlated well with other useful experimental spectroscopic properties, such as the pyrrole proton NMR shifts and the magnetic susceptibilities.[15] Therefore, the quantitative relationship with the Fe−N bond lengths may help structural investigations of the $S = {}^3/_2$ and ${}^5/_2$ heme proteins using a number of experimental techniques.

It is also interesting to note that among the $S = {}^3/_2$ ferric porphyrins investigated here, which include three porphyrin coordination states (four-, five-, and six-coordinate) and three common porphyrin conformations (planar, ruffled, and saddled), there are only two general trends in the porphyrin ^{13}C NMR hyperfine shifts based on the experimental and computational results, and these trends were found to depend on the porphyrin conformation, not the coordination state: $\delta_{hf}^{C\alpha} < \delta_{hf}^{C\beta} < \delta_{hf}^{Cm}$ for planar and ruffled

10.1021/ja9006723 CCC: $40.75 © 2009 American Chemical Society

Table 1. Mössbauer, NMR, Geometric, and Electronic Properties in $S = {}^3/_2$ and ${}^5/_2$ Iron Porphyrins[a]

complex		S	R_{FeN} (Å)	ΔE_Q (mm/s)	δ_{Fe} (mm/s)	$\delta_{hf}^{H\beta}$ (ppm)	$\delta_{hf}^{HC\alpha}$ (ppm)	$\delta_{hf}^{C\alpha}$ (ppm)	$\delta_{hf}^{C\beta}$ (ppm)	δ_{hf}^{Cm} (ppm)	refs
1 [Fe(TipsiPP)]$CB_{11}H_6Br_6$	exptl	${}^3/_2$	1.944	5.16	0.33	−90.2					3
four-coordinate	calcd	${}^3/_2$		4.97	0.24	−94.2	/	−509.9	−195.1	−100.6	
planar		${}^5/_2$		4.10	0.27	−29.4	/	1795.1	1213.2	−350.5	
2 Fe(OEP)(3-ClPy)	exptl	${}^3/_2$	1.979	3.23	0.36						16, 17
five-coordinate	calcd	${}^3/_2$		2.82	0.33	/	26.7, 6.3	−470.2	−38.4	89.7	
planar		${}^5/_2$		1.98	0.34	/	56.3, 45.3	1304.6	1023.8	−46.8	
3 Fe(TMCP)(H_2O)(EtOH)	exptl	${}^3/_2$	1.950	3.79	0.35	−44.2					13
six-coordinate	calcd	${}^3/_2$		3.65	0.32	−55.1	/	−313.7	−177.0	−28.4	
ruffled		${}^5/_2$		3.16	0.34	27.1	/	1418.5	1185.8	−31.8	
4 [Fe(T^{i}PrP)$(THF)_2$]ClO_4	exptl	${}^3/_2$	1.967	3.71	0.34	−61.1		−272.8	−110.5	−28.3	5, 12
six-coordinate	calcd	${}^3/_2$		3.33	0.35	−59.0	/	−299.7	−207.7	−44.4	
ruffled		${}^5/_2$		2.81	0.35	25.2	/	1588.4	1013.5	−92.0	
5 Fe(OETPP)ClO_4	exptl	${}^3/_2$	1.963				32.5, 2.8				4, 11
five-coordinate	calcd	${}^3/_2$		3.31	0.40	/	22.2, 0.0	117.3	17.4	−120.5	
saddled		${}^5/_2$		3.27	0.40	/	205.5, 25.7	1834.8	−371.7	−1854.5	
6 [Fe(OETPP)$(4\text{-}CNPy)_2$]ClO_4	exptl	${}^3/_2$	1.975	3.03	0.57		31.6, 3.5	318.8	133.1	−388.9	4, 7, 9, 10
six-coordinate	calcd	${}^3/_2$		2.67	0.60	/	30.1, 1.6	201.3	11.1	−252.1	
saddled		${}^1/_2$		3.51	0.43	/	6.3, 3.1	72.9	−50.8	158.5	
7 [Fe(TipsiPP)]CF_3SO_3	exptl	${}^5/_2$	2.053								3
five-coordinate	calcd	${}^5/_2$		1.07	0.46	59.3	/	1171.5	1140.6	178.7	
planar		${}^3/_2$		3.70	0.54	−10.4	/	−106.4	−226.5	60.6	
8 Fe(OETPP)Cl	exptl	${}^5/_2$	2.040	0.95	0.35		31.7, 15.9				4, 14
five-coordinate	calcd	${}^5/_2$		0.71	0.42	/	19.0, 10.1	602.8	1004.6	314.2	
saddled		${}^3/_2$		1.88	0.48	/	3.1, 0.0	144.3	44.4	−87.2	

[a] TipsiPP = 5,10,15,20-tetrakis(2′,6′-bis(triisopropylsiloxy)phenylporphyrinato, OEP = 2,3,7,8,12,13,17,18-octaethylporphyrinato, TMCP = 5,10,15,20-tetramethylchiroporphyrinato, T^{i}PrP = 5,10,15,20-tetraisopropylporphyrinato, OETPP = 2,3,7,8,12,13,17,18-octaethyl-5,10,15,20-tetraphenylporphyrinato. Temperatures for the Mössbauer and NMR results are listed in Table S1.

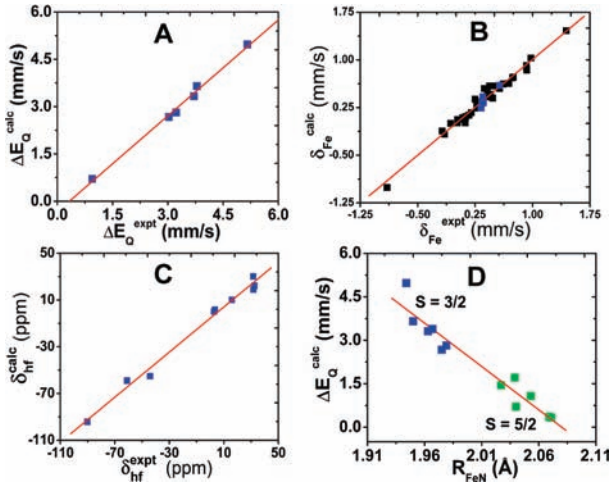

Figure 1. (A) Computed Mössbauer quadrupole splittings vs experimental data. (B) Calculated Mössbauer isomer shifts vs experimental results. (C) Calculated ^{1}H NMR hyperfine shifts vs experimental data. (D) Relationship between ΔE_Q and R_{FeN}. Blue and green data points are from this work and black data points are from previous work.[18,20]

complexes and the opposite trend of $\delta_{hf}^{C\alpha} > \delta_{hf}^{C\beta} > \delta_{hf}^{Cm}$ for saddled ones (see Table 1). This indicates an important effect of the porphyrin conformation on the electronic structures, as discussed below. Previous work[4,8,19] suggested that the relative ordering of $d_{xz/yz}$ (or d_π) versus d_{xy} can affect the ^{13}C NMR hyperfine shift trends in the ruffled and saddled $S = {}^3/_2$ iron porphyrins. Unfortunately, controversial results were obtained in the past.[4,8,19] To resolve this problem and understand the new observations found here for the ^{13}C NMR hyperfine shift trends in these intermediate-spin ferric complexes with a greater variety of porphyrin structures, we investigated all of the wavefunctions from the above successful calculations. As shown in Figure 2A,E,I,M and Figures S3A and S4A, a common outcome for all of these $S = {}^3/_2$ complexes is that $d_{x^2-y^2}$ has the highest energy, supporting previous work.[1,4,8,19] However, as a result of the current comprehensive investigation, more possibilities than previously known for the frontier MO orderings were discovered:

(1) $d_{x^2-y^2} > d_\pi > d_{xy} > d_{z^2}$ for complexes **1**, **3**, and **4** (see Figure 2A−D, Figure S3, and Figure S4, respectively);
(2) $d_{x^2-y^2} > d_{z^2} > d_\pi > d_{xy}$ for complex **2** (see Figure 2E−H);
(3) $d_{x^2-y^2} > d_{xy} > d_\pi > d_{z^2}$ for complex **5** (see Figure 2I−L);
(4) $d_{x^2-y^2} > d_{xy} > d_{z^2} > d_\pi$ for complex **6** (see Figure 2M−P).

On the basis of these results, it seems that the MO ordering does not depend on the coordination state. In contrast, the porphyrin conformation was found to play an important role, as shown in Figure 2 and Figures S3 and S4. This is consistent with the above observations on the ^{13}C NMR results. Of particular interest is that though altogether a number of different frontier MO orderings were discovered here, there are only two orderings that concern the iron d_π and d_{xy} orbitals: $d_\pi > d_{xy}$ in planar and ruffled complexes and the opposite trend of $d_\pi < d_{xy}$ in the saddled ones (Figure 2). This kind of porphyrin conformation dependence is again the same as with the porphyrin ^{13}C NMR hyperfine shifts, suggesting that the porphyrin conformation affects the relative ordering of the d_π and d_{xy} orbitals, which are responsible for the observed porphyrin ^{13}C NMR results. This occurs because among the three types of occupied iron d orbitals (d_π, d_{xy}, and d_{z^2}), only the d_π and d_{xy} orbitals make significant contributions to the spin densities in the porphyrin ring, while the d_{z^2} orbital mainly influences the axial ligands. Another interesting new observation is that the d_{z^2} ordering depends on the Fe−N distance. As shown in Figure 2 and Figures S3 and S4, among the planar and ruffled $S = {}^3/_2$ complexes, d_{z^2} usually has the lowest energy when R_{FeN} is small, as a result of the weaker interaction along the z axis in comparison with the stronger ones in the xy plane from the shorter Fe−N contacts. However, when R_{FeN} is long (≥1.975 Å), d_{z^2} is higher than d_π as usual. The same kind of dependence of d_{z^2} on R_{FeN} was also found for the saddled $S = {}^3/_2$ porphyrins (see Figure 2).

Overall, the results presented here should facilitate future investigations of related iron porphyrins and heme proteins.

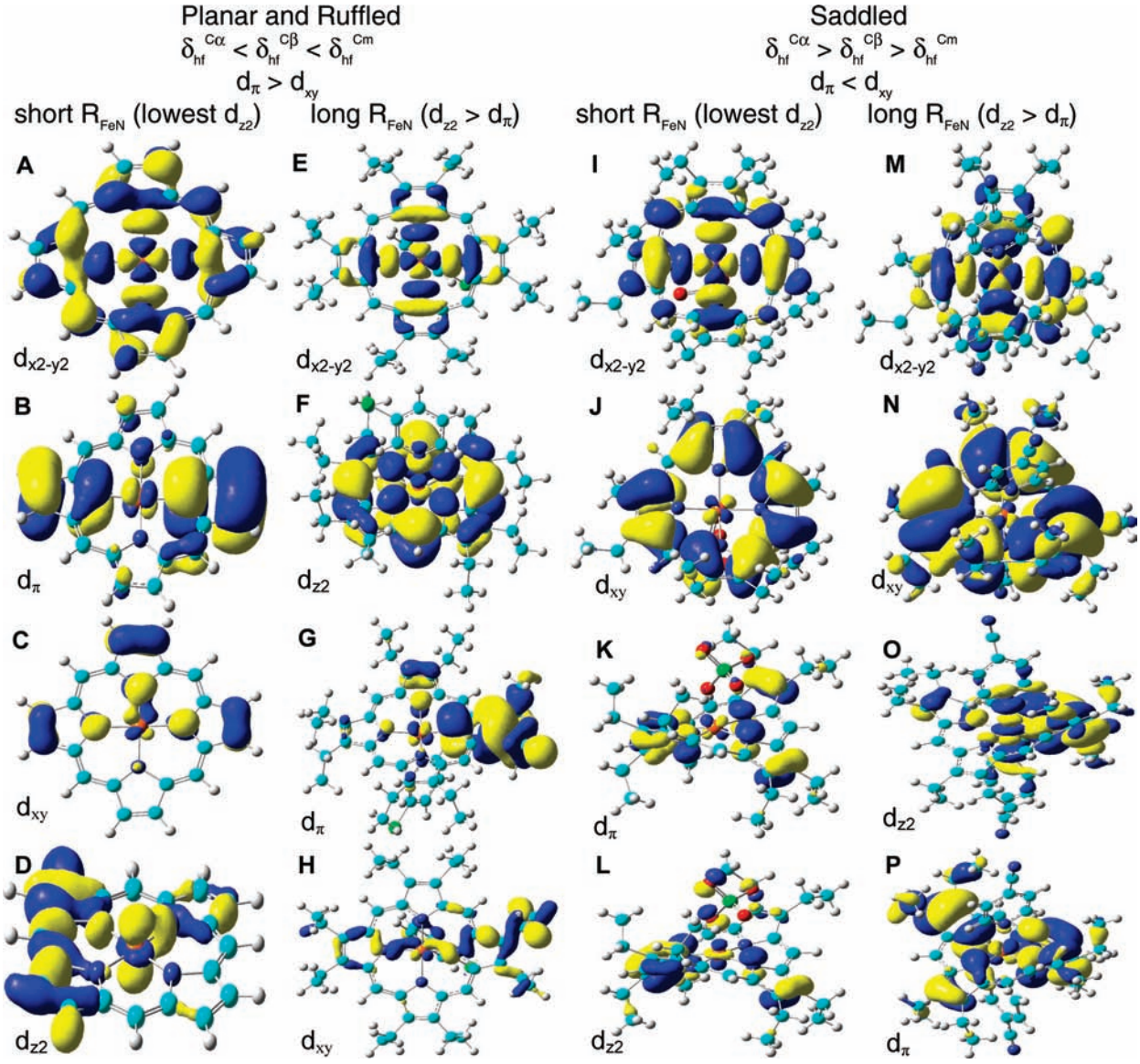

Figure 2. Summary of the structural dependence of porphyrin ^{13}C NMR trends and MO orderings and isosurface representations of (A) α-LUMO, (B) α-HOMO−2, (C) *β*-HOMO−3, and (D) α-HOMO−12 for **1**; (E) α-LUMO, (F) α-HOMO−1, (G) α-HOMO−2, and (H) α-HOMO−12 for **2**; (I) α-LUMO+1, (J) *β*-HOMO, (K) α-HOMO−2, and (L) α-HOMO−5 for **5**; and (M) α-LUMO+2, (N) α-HOMO, (O) α-HOMO−2, and (P) α-HOMO−3 for **6**. The contour values are ±0.02, 0.02, 0.04, 0.04, 0.02, 0.02, 0.02, 0.04, 0.02, 0.02, 0.04, 0.04, 0.02, 0.01, 0.02, and 0.02 au, respectively.

Acknowledgment. This work was supported in part by NSF EPSCoR Award OIA-0556308 and NIH Grant GM-085774.

Supporting Information Available: Computational details and other experimental information (Tables S1−S2 and Figures S1−S4). This material is available free of charge via the Internet at http://pubs.acs.org.

References

(1) Weiss, R.; Gold, A.; Terner, J. *Chem. Rev.* **2006**, *106*, 2550–2579.
(2) Zeng, Y. H.; Caignan, G. A.; Bunce, R. A.; Rodriguez, J. C.; Wilks, A.; Rivera, M. *J. Am. Chem. Soc.* **2005**, *127*, 9794–9807.
(3) Fang, M.; Wilson, S. R.; Suslick, K. S. *J. Am. Chem. Soc.* **2008**, *130*, 1134–1135.
(4) Nakamura, M. *Coord. Chem. Rev.* **2006**, *250*, 2271–2294.
(5) Hoshino, A.; Ohgo, Y.; Nakamura, M. *Inorg. Chem.* **2005**, *44*, 7333–7344.
(6) Yatsunyk, L. A.; Shokhirev, N. V.; Walker, F. A. *Inorg. Chem.* **2005**, *44*, 2848–2866.
(7) Yatsunyk, L. A.; Walker, F. A. *Inorg. Chem.* **2004**, *43*, 757–777.
(8) Sakai, T.; Ohgo, Y.; Ikeue, T.; Takahashi, M.; Takeda, M.; Nakamura, M. *J. Am. Chem. Soc.* **2003**, *125*, 13028–13029.
(9) Ikeue, T.; Ohgo, Y.; Ongayi, O.; Vicente, M. G. H.; Nakamura, M. *Inorg. Chem.* **2003**, *42*, 5560–5571.
(10) Ikeue, T.; Ohgo, Y.; Yamaguchi, T.; Takahashi, M.; Takeda, M.; Nakamura, M. *Angew. Chem., Int. Ed.* **2001**, *40*, 2617–2620.
(11) Barkigia, K. M.; Renner, M. W.; Fajer, J. *J. Porphyrins Phthalocyanines* **2001**, *5*, 415–418.
(12) Ikeue, T.; Saitoh, T.; Yamaguchi, T.; Ohgo, Y.; Nakamura, M.; Takahashi, M.; Takeda, M. *Chem. Commun.* **2000**, 1989–1990.
(13) Simonato, J. P.; Pecaut, J.; Le Pape, L.; Oddou, J. L.; Jeandey, C.; Shang, M.; Scheidt, W. R.; Wojaczynski, J.; Wolowiec, S.; Latos-Grazynski, L.; Marchon, J. C. *Inorg. Chem.* **2000**, *39*, 3978–3987.
(14) Schunemann, V.; Gerdan, M.; Trautwein, A. X.; Haoudi, N.; Mandon, D.; Fischer, J.; Weiss, R.; Tabard, A.; Guilard, R. *Angew. Chem., Int. Ed.* **1999**, *38*, 3181–3183.
(15) Reed, C. A.; Guiset, F. *J. Am. Chem. Soc.* **1996**, *118*, 3281–3282.
(16) Scheidt, W. R.; Geiger, D. K.; Lee, Y. J.; Reed, C. A.; Lang, G. *Inorg. Chem.* **1987**, *26*, 1039–1045.
(17) Debrunner, P. G. In *Iron Porphyrins*; Lever, A. B. P., Gray, H. B., Eds.; VCH Publishers: New York, 1989; Vol. 3, pp 139−234.
(18) (a) Zhang, Y.; Mao, J.; Oldfield, E. *J. Am. Chem. Soc.* **2002**, *124*, 7829–7839. (b) Zhang, Y.; Mao, J.; Godbout, N.; Oldfield, E. *J. Am. Chem. Soc.* **2002**, *124*, 13921–13930.
(19) Cheng, R. J.; Wang, Y. K.; Chen, P. Y.; Han, Y. P.; Chang, C. C. *Chem. Commun.* **2005**, 1312–1314.
(20) (a) Zhang, Y.; Gossman, W.; Oldfield, E. *J. Am. Chem. Soc.* **2003**, *125*, 16387–16396. (b) Zhang, Y.; Oldfield, E. *J. Phys. Chem. B* **2003**, *107*, 7180–7188. (c) Zhang, Y.; Oldfield, E. *J. Phys. Chem. A* **2003**, *107*, 4147–4150. (d) Zhang, Y.; Oldfield, E. *J. Am. Chem. Soc.* **2004**, *126*, 4470–4471. (e) Zhang, Y.; Oldfield, E. *J. Am. Chem. Soc.* **2004**, *126*, 9494–9495.
(21) (a) Mao, J.; Zhang, Y.; Oldfield, E. *J. Am. Chem. Soc.* **2002**, *124*, 13911–13930. (b) Zhang, Y.; Oldfield, E. *J. Am. Chem. Soc.* **2008**, *130*, 3814–3823.
(22) See the Supporting Information for computational details.

JA9006723